Published February 11, 2008

Importin-β and the small guanosine triphosphatase Ran mediate chromosome loading of the human chromokinesin Kid

Kiyoshi Tahara,[1] Masatoshi Takagi,[1] Miho Ohsugi,[2] Takefumi Sone,[3] Fumiko Nishiumi,[3] Kazuhiro Maeshima,[1] Yasuomi Horiuchi,[2] Noriko Tokai-Nishizumi,[2] Fumio Imamoto,[3] Tadashi Yamamoto,[2] Shingo Kose,[1] and Naoko Imamoto[1]

[1]Cellular Dynamics Laboratory, Discovery Research Institute, Institute of Physical and Chemical Research, Wako, Saitama, 351-0198, Japan
[2]Division of Oncology, Department of Cancer Biology, Institute of Medical Science, University of Tokyo, Tokyo 108-8639, Japan
[3]Laboratory of Molecular Biology, Research Institute for Microbial Diseases, Osaka University, Suita, Osaka 565-0871, Japan

Nucleocytoplasmic transport factors mediate various cellular processes, including nuclear transport, spindle assembly, and nuclear envelope/pore formation. In this paper, we identify the chromokinesin human kinesin-like DNA binding protein (hKid) as an import cargo of the importin-α/β transport pathway and determine its nuclear localization signals (NLSs). Upon the loss of its functional NLSs, hKid exhibited reduced interactions with the mitotic chromosomes of living cells. In digitonin-permeabilized mitotic cells, hKid was bound only to the spindle and not to the chromosomes themselves. Surprisingly, hKid bound to importin-α/β was efficiently targeted to mitotic chromosomes. The addition of Ran–guanosine diphosphate and an energy source, which generates Ran–guanosine triphosphate (GTP) locally at mitotic chromosomes, enhanced the importin-β–mediated chromosome loading of hKid. Our results indicate that the association of importin-β and -α with hKid triggers the initial targeting of hKid to mitotic chromosomes and that local Ran-GTP–mediated cargo release promotes the accumulation of hKid on chromosomes. Thus, this study demonstrates a novel nucleocytoplasmic transport factor–mediated mechanism for targeting proteins to mitotic chromosomes.

Introduction

The selective transport of large populations of molecules between the nucleus and cytoplasm is organized by a series of interactions between cargo and carrier molecules regulated by the small GTPase Ran (Stewart, 2007). One such carrier molecule, importin-β, was initially identified as a nuclear import mediator of classical NLS-containing proteins in association with the adaptor molecule importin-α (Adam and Gerace, 1991; Gorlich et al., 1994, 1995; Chi et al., 1995; Imamoto et al., 1995a,b). In this well-characterized transport pathway, importin-β forms an import complex with its cargo in the cytoplasm via an interaction with importin-α, which then passes through a nuclear pore. In the nucleus, Ran-GTP binds to importin-β, triggering disassembly of the import complex and cargo release. Ran-GTP–bound importin-β then returns to the cytoplasm, whereas importin-α forms a trimeric complex with another member of the importin-β family, cellular apoptosis susceptibility (CAS)/exportin-2, in conjunction with Ran-GTP, to exit the nucleus (Kutay et al., 1997). The conversion of Ran-GTP to Ran-GDP in the cytoplasm by Ran GTPase-activating protein (GAP) releases the importins, thereby allowing them to participate in subsequent import cycles. Cargo recognition and cargo release are restricted to the cytoplasm and nucleus because each process is critically dependent on Ran-GTP, whose cytoplasmic concentration is low because of the cytoplasmic localization of RanGAP and whose nuclear concentration is high because of the nuclear localization of the Ran guanine nucleotide exchange factor regulator of chromosome condensation 1 (RCC1; Melchior, 2001). Such spatially and temporally organized interactions between carrier and cargo are the basis of all importin-β–based transport pathways, including those that do not involve adaptor

Correspondence to Naoko Imamoto: nimamoto@riken.jp

Abbreviations used in this paper: CAS, cellular apoptosis susceptibility; FLIP, fluorescence loss in photobleaching; GAP, GTPase-activating protein; hKid, human kinesin-like DNA binding protein; RCC1, regulator of chromosome condensation 1; SAF, spindle assembly factor; wt, wild type.

The online version of this paper contains supplemental material.

The Journal of Cell Biology, Vol. 180, No. 3, February 11, 2008 493–506
http://www.jcb.org/cgi/doi/10.1083/jcb.200708003

Supplemental Material can be found at:
http://jcb.rupress.org/cgi/content/full/jcb.200708003/DC1

Published February 11, 2008

molecules like importin-α and those that are mediated by other families of importin-β–related proteins (Gorlich and Kutay, 1999; Imamoto, 2000; Macara, 2001).

Several recent studies have revealed the importance of Ran-GTP–regulated interactions between mitotic effectors and transport carriers in mitotic progression (Sazer and Dasso, 2000; Wilde et al., 2001; Hetzer et al., 2002; Harel and Forbes, 2004; Ciciarello et al., 2007). For example, spindle assembly factors (SAFs) harboring basic NLSs, like TPX2 or NuMA, are inactive when bound to importin-α and -β but the binding of Ran-GTP to importin-β liberates and activates these factors, triggering spindle formation (Gruss et al., 2001; Nachury et al., 2001; Wiese et al., 2001). This activation is believed to occur in the vicinity of the chromosomes because of the local buildup of Ran-GTP through the action of chromosome-bound RCC1 (Kalab et al., 2002, 2006; Li and Zheng, 2004; Caudron et al., 2005). Extensive searches for Ran-GTP–regulated SAFs have identified XCTK2 (Ems-McClung et al., 2004), Xnf7 (Maresca et al., 2005), NuSAP (Ribbeck et al., 2006, 2007), Rae1 (Blower et al., 2005), and HURP (Koffa et al., 2006; Sillje et al., 2006). More recently, MEL-28/ELYS has been suggested to be a Ran effector that is important for the assembly of the nuclear envelope and nuclear pore complexes (Rasala et al., 2006; Franz et al., 2007). All of these factors are localized to the nucleus during interphase and they bind importin-β, either directly or indirectly, via adaptor molecules. In all cases examined, importin-β negatively regulates its cargo either by inhibiting its activity or binding its partner molecules. The role of importin-β in mitosis indicates that it does not merely function as a carrier molecule for nuclear import but also as a regulator of its cargo proteins.

Yeast two-hybrid screening using importin-β as bait picked up the chromokinesin human kinesin-like DNA binding protein (hKid)/Kinesin-10 (unpublished data), whereas complementary screening using hKid as bait picked up importin-α (unpublished data). hKid is a plus end–directed microtubule-based motor with a DNA binding domain that is involved in generating the polar ejection force that pushes the chromosome arms away from the spindle poles toward the metaphase plate (Tokai et al., 1996; Antonio et al., 2000; Funabiki and Murray, 2000; Levesque and Compton, 2001; Tokai-Nishizumi et al., 2005). The depletion of Kid in meiotic systems causes chromosome misalignment (Antonio et al., 2000; Funabiki and Murray, 2000), whereas perturbation of Kid activity in somatic cultured cells causes a loss of chromosome oscillation during prometaphase and metaphase (Levesque and Compton, 2001; Tokai-Nishizumi et al., 2005). Besides its apparent localization on mitotic chromosomes, Kid is also localized on the spindle via its microtubule binding activity, which is regulated by cdc2-mediated phosphorylation (Ohsugi et al., 2003). Because hKid exhibits nuclear localization (Tokai et al., 1996), nucleocytoplasmic transport factors were assumed to regulate its function in mitosis, and importin-α/β was shown to inhibit the microtubule binding activity of hKid in vitro (Trieselmann et al., 2003). However, it is unclear how the regulatory effects of the nucleocytoplasmic transport system actually contribute to the mitotic function of hKid.

In this paper, we identify the NLSs of hKid and examine how the loss of its NLSs affects its behavior during mitosis in living cells. FRAP and fluorescence loss in photobleaching (FLIP) analyses revealed that the interaction between hKid and mitotic chromosomes is weakened by the loss of its functional NLSs. In digitonin-permeabilized cells, the association of hKid with importin-β via importin-α triggered the initial targeting of hKid to mitotic chromosomes, and local Ran-GTP–mediated cargo release promoted the accumulation of hKid on the chromosomes. These observations indicate that the regulatory effects of importin-β on mitosis are not restricted to simple inhibition, but are spatially regulated interactions that mediate chromosome loading of hKid. Our results suggest the existence of a novel active mechanism by which certain molecules are targeted to mitotic chromosomes in a nucleocytoplasmic transport factor–mediated manner.

Results

hKid contains two basic NLSs that interact with importin-α and -β

hKid was previously shown to contain at least two NLSs that bind to importin-β either directly or indirectly in a Ran-GTP–sensitive manner (Trieselmann et al., 2003). We assessed the binding of hKid to various transport receptors using bacterially expressed full-length recombinant hKid. As shown in Fig. 1 A, purified recombinant hKid did not bind importin-β directly but associated with importin-β in the presence of importin-α. Using a digitonin-permeabilized cell-free transport assay (Adam et al., 1990), hKid was found to migrate into the nucleus only in the presence of importin-α, importin-β, and Ran, which is consistent with the behavior of proteins that migrate into the nucleus via the conventional importin-α/β pathway (Fig. S1, available at http://www.jcb.org/cgi/content/full/jcb.200708003/DC1).

Full-length hKid bound importin-α directly; however, this binding was abolished when critical residues of importin-α, which are responsible for its association with conventional basic NLSs, were mutated (ED mutant; Conti et al., 1998; Gruss et al., 2001; Fig. 1 B), suggesting that hKid contains conventional basic NLS(s). Thus, we next focused on two basic clusters within hKid (Fig. 1 D, ^{400}KRAR^{403} and ^{556}RKRKL^{560}) that are conserved among the Kid homologues in various species and examined their requirement for nuclear localization activity. As shown in Fig. 1 C, mutations in either cluster (^{400}AAAA^{403} or ^{556}AAGAA^{560}) did not abolish the nuclear localization of hKid or its ability to bind importin-α/β, whereas mutations in both clusters did (not depicted). These results indicate that hKid possesses two basic NLSs, each of which is sufficient as a functional NLS, and that both NLSs are recognized by importin-α/β. It should be noted that the two NLSs reside outside the known functional domains. One lies in between the kinesin-like motor domain and coiled-coil domain, whereas the other lies in between the coiled-coil domain and DNA binding domain (Fig. 1 D). Consistent with this, mutations within the NLSs affected neither the microtubule nor DNA binding properties of hKid (see following paragraph). Based on these results, we next examined the mitotic behavior/function of hKid.

Published February 11, 2008

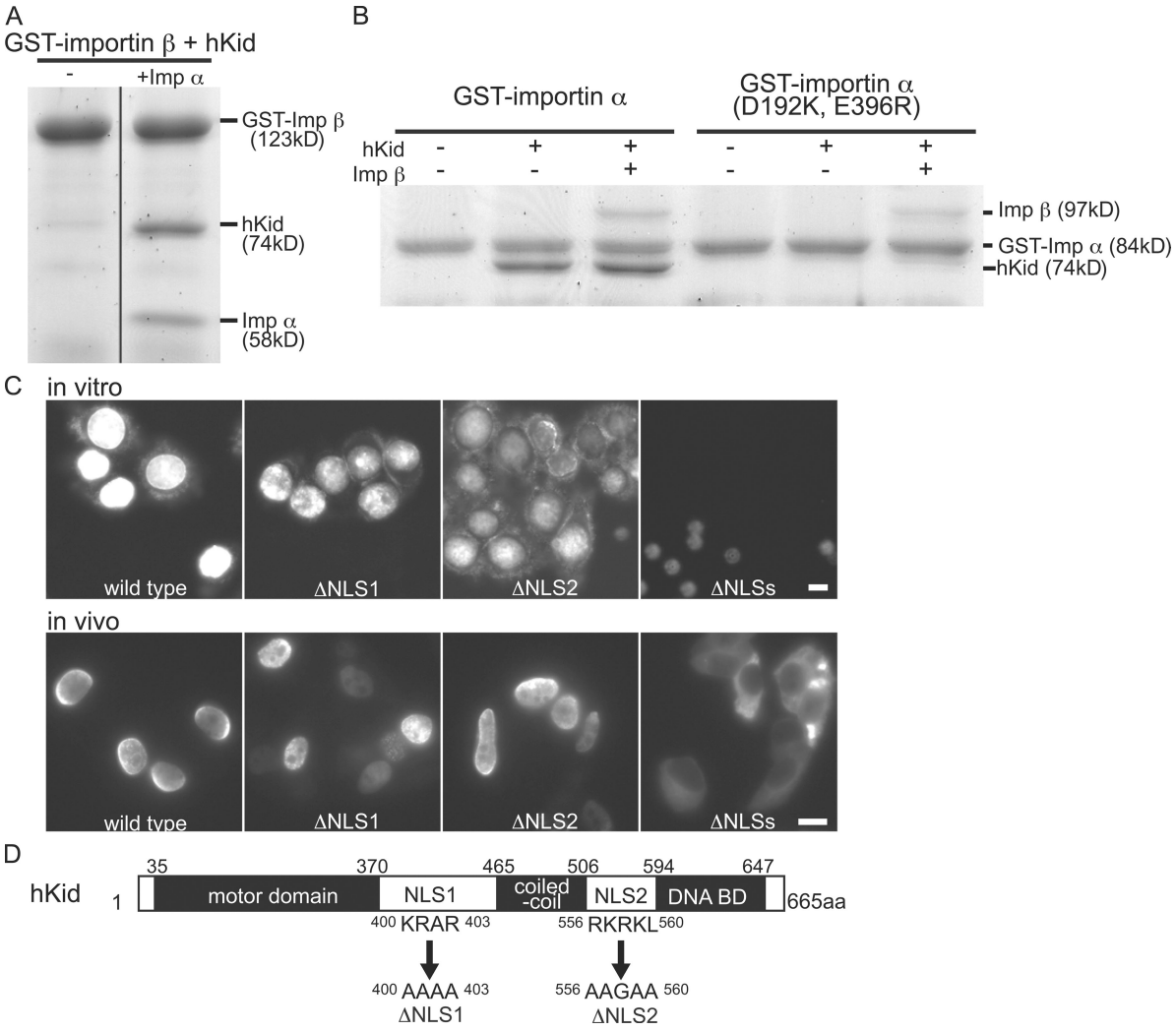

Figure 1. **hKid possesses two functional NLSs that bind importin-β via importin-α.** (A) 30 pmol of recombinant GST–importin-β, 60 pmol FLAG-hKid, and 30 pmol importin-α were incubated in 50 µl of solution and then pulled down with glutathione-Sepharose beads. The bound proteins were analyzed by SDS-PAGE followed by Coomassie brilliant blue staining. hKid bound importin-β in the presence of importin-α. (B) 20 pmol of recombinant GST–importin-α or its ED mutant (defective in basic NLS binding) was incubated with 40 pmol FLAG-hKid, 40 pmol importin-β, or both in 50 µl of solution and then pulled down with glutathione-Sepharose beads. Coomassie brilliant blue staining of the bound proteins analyzed by SDS-PAGE is shown. Importin-α bound hKid directly, whereas the mutant version of importin-α did not bind hKid. Importin-β binding was unaffected by the mutations introduced in importin-α. (C, top) Nuclear migration of 0.4 µM of recombinant FLAG-hKid was examined in digitonin-permeabilized HeLa cells in the presence of 0.4 µM importin-α, 0.4 µM importin-β, 4 µM Ran-GDP, and an energy source. (C, bottom) Localization of EGFP-hKid in HeLa cells 3 h after nuclear injection of the expression plasmid. Mutations in both NLSs abolished the nuclear localization of hKid. Bars, 10 µm. (D) Schematic diagram of hKid. The positions of the two NLSs where mutations were introduced are indicated by arrows.

Removal of the functional NLSs in hKid reduces its interaction with mitotic chromosomes in living cells

To determine whether mitotic function of hKid is regulated by nucleocytoplasmic transport factors, we examined the contribution of each NLS to the mitotic behavior of hKid in living cells. For this purpose, cell lines stably expressing fluorescently tagged wild-type (wt) hKid (Venus–wt hKid) or mutant hKid defective in both its NLSs (Venus–ΔNLSs hKid) were established. Because the overexpression of hKid is highly cytotoxic and induces mitotic abnormalities (Ohsugi et al., 2003; this study), an Flp–FRT recombination system was used that allows for the selection of cells carrying only one or a few copies of an objective gene integrated into defined genomic loci (Yahata et al., 2005; see Materials and methods). The cell lines expressed Venus–wt hKid and –ΔNLSs hKid at a level below or nearly equal to that of endogenous hKid (Fig. 2 B), respectively, without affecting the cell cycle/mitotic profile. We were unable to establish lines expressing higher levels of Venus–wt hKid, probably because overexpression of wt hKid is more toxic for cells than overexpression of mutant hKid defective in its NLSs.

As shown in Fig. 2 A, both Venus–wt hKid and –ΔNLSs hKid were localized predominantly to the mitotic chromosomes and also to the spindle at lower levels, similar to those of endogenous hKid (see Fig. 7). The spindle signal for Venus–ΔNLSs hKid was stronger than that for Venus–wt hKid (Fig. 2 A). The dynamics of these two proteins were next examined by FRAP within a small region of the mitotic chromosomes (Fig. 2 B and

Published February 11, 2008

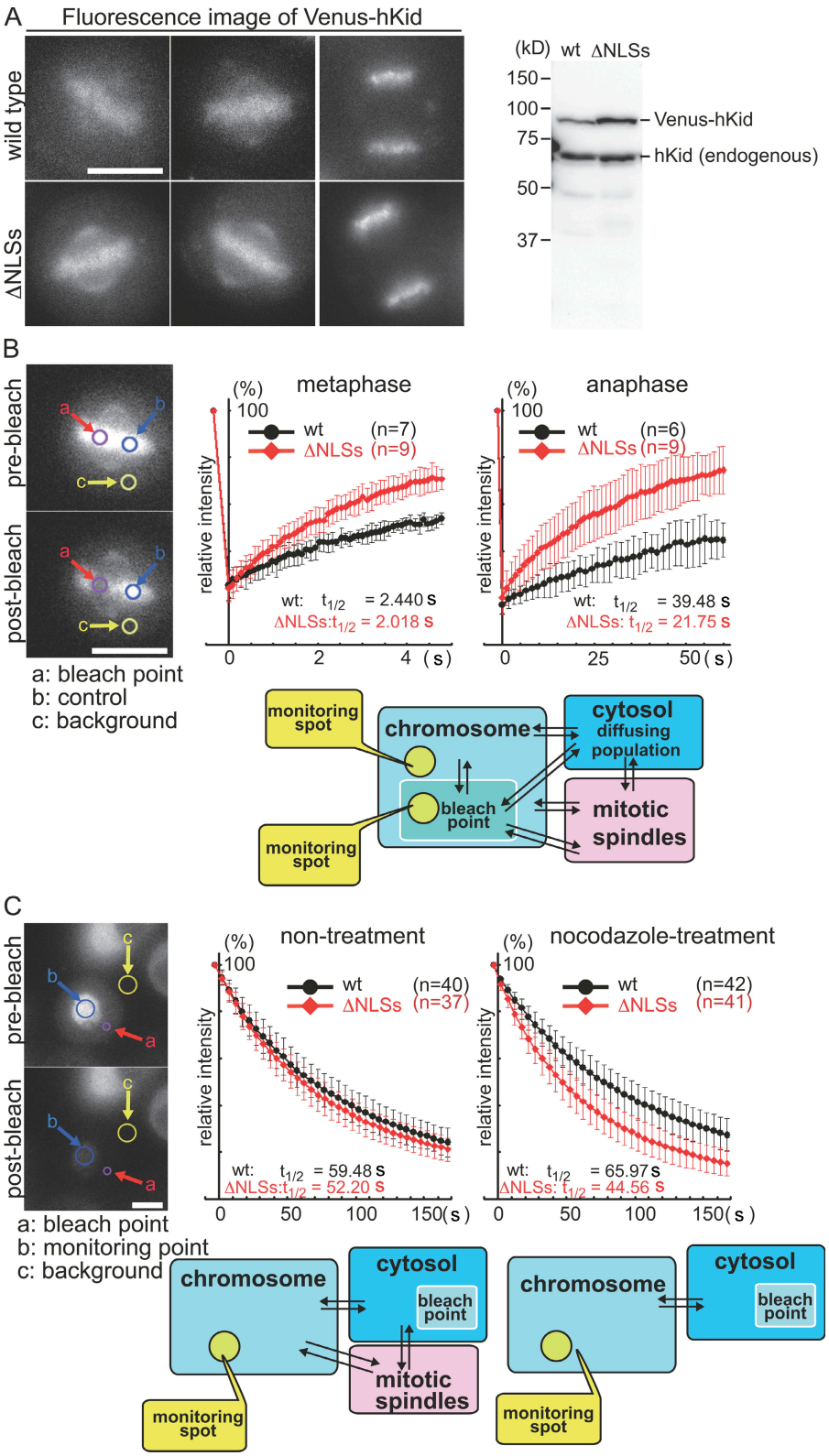

Figure 2. **Loss of the functional NLSs in hKid reduces its interaction with mitotic chromosomes in living cells.** (A) Representative images of Venus–wt hKid and Venus–ΔNLSs hKid in stably transformed live HeLa cells. Cells in metaphase (left) and anaphase (right) are shown. To compare the localization signals in the cells, the fluorescent intensities were digitally compensated. The actual fluorescent intensity of Venus–ΔNLSs hKid was much higher than that of Venus–wt hKid. Bar, 10 μm. (B) FRAP analysis of Venus–wt hKid or Venus–ΔNLSs hKid on chromosomes. The mean intensity of a bleached chromosomal spot (a), a nonbleached chromosomal spot (b, control), and a nonchromosomal spot (c, background) were measured over time (micrographs). All FRAP measurements were plotted as a function of time (graphs). The mean values and their standard deviations from six to nine cells are plotted. The diagram below depicts our experimental design. All possibilities for the replacement and turnover of hKid between each compartment are indicated by arrows. Bar, 10 μm. (C) FLIP analysis of Venus–wt hKid or Venus–ΔNLSs hKid in the presence (−nocodazole) or absence (+nocodazole) of a mitotic spindle. A spot outside the chromosomes and mitotic spindle (a) was irradiated, and the mean intensities of a chromosome spot (b) and a spot outside the cells (c, background) were measured before and during irradiation (micrographs). All FLIP measurements were plotted as a function of time (graphs). The mean values and their standard deviations from 37–42 cells are plotted. The diagrams below depict our experimental design. Arrows indicate putative replacements and the turnover of hKid between each compartment. Each $t_{1/2}$ value was calculated from the best-fit curve as described in Materials and methods. Bar, 10 μm.

Fig. S2, available at http://www.jcb.org/cgi/content/full/jcb.200708003/DC1). Chromosome-bound hKid was highly dynamic during prometaphase and metaphase, with the recovery of fluorescence occurring within seconds (Fig. 2 B, left graph). Meanwhile, the mobility of chromosome-bound hKid was greatly reduced during anaphase, as the recovery of the fluorescence required nearly 1 min (Fig. 2 B, right graph). Both in metaphase and anaphase, the recovery of Venus–ΔNLSs hKid was quicker and more efficient than that of Venus–wt hKid, indicating that the turnover, as well as the mobile fraction, of chromosome-bound hKid increases upon the loss of its functional NLSs. Quantitatively, Venus–wt hKid displayed a $t_{1/2}$ of 2.4 s with 63%

Published February 11, 2008

recovery in metaphase and a $t_{1/2}$ of 39 s with 61% recovery in anaphase, whereas Venus–ΔNLSs hKid displayed a $t_{1/2}$ of 2.0 s with 83% recovery in metaphase and a $t_{1/2}$ of 22 s with 83% recovery in anaphase (Fig. 2 B and Fig. S2). At present, we do not know exactly how hKid moves in mitotic cells although, conceptually, the hKid in the bleached area could be replaced laterally by hKid from a nonbleached chromosomal area, directly by hKid from the cytosolic pool, or by hKid from the mitotic spindle (Fig. 2 B, diagram).

The quantitative data suggested that the NLSs of hKid affect its interaction with mitotic chromosomes. Thus, to evaluate the contribution of the mitotic spindle to this process, we attempted to examine the dynamics of hKid in cells treated with nocodazole, a microtubule depolymerizing agent. In the absence of a mitotic spindle, the mitotic chromosomes began to move around within the cells, making it difficult to monitor a small bleached chromosomal area over time. Therefore, we used FLIP analysis instead of FRAP. A cytoplasmic region outside the chromosomes and spindle was bleached repeatedly and the decline in fluorescence at the mitotic chromosomes was monitored. As shown in Fig. 2 C (right graph), the fluorescence of chromosome-bound Venus–ΔNLSs hKid declined more rapidly than that of Venus–wt hKid in the absence of a mitotic spindle. Quantitatively, Venus–wt hKid displayed a $t_{1/2}$ of 66 s, whereas Venus–ΔNLSs hKid displayed a $t_{1/2}$ of 45 s. This indicates that the NLSs of hKid contribute to the strength of its interaction with mitotic chromosomes regardless of the presence of spindle microtubules. When the behavior of chromosome-bound Venus–wt hKid and –ΔNLSs hKid was compared by FLIP analysis in the presence of spindle microtubules (Fig. 2 C, left graph), the differences shown in Fig. 2 were not detected (see Discussion).

Binding of hKid to importin-β via importin-α represses spindle binding but facilitates chromosome targeting of hKid

To make sense of the observation in the previous section, we examined the mitotic behavior of hKid in digitonin-permeabilized mitotic cells using purified recombinant proteins. As shown in Fig. 3 A (first column), in permeabilized mitotic cells incubated with purified recombinant hKid, hKid was bound only to the mitotic spindles, and not to the mitotic chromosomes, despite its DNA binding domain. Surprisingly, when hKid was incubated together with importin-α and -β, it was efficiently targeted to the mitotic chromosomes (Fig. 3 A, second column), whereas targeting to the spindle was reduced (Fig. 3 A, compare the first and second columns). The addition of Q69L Ran-GTP, a mutant Ran defective in GTP hydrolysis (Klebe et al., 1995) that disrupts the binding of cargo to importin-β, reversed the effects of importin-α and -β (Fig. 3 A, third column). Accordingly, ΔNLSs hKid was able to bind the spindle microtubules regardless of whether importin-α and -β were present (Fig. 3 A, fourth column). An excess amount of each recombinant protein was incubated with the permeabilized cells; therefore, the reduction in spindle or chromosome binding observed under each condition should represent the inability of hKid to bind either structures, respectively, rather than an indirect effect, such as the consequence of sequestering hKid. We thus concluded that the binding of importin-α and -β to hKid targets hKid to chromosomes and disrupts its ability to bind the mitotic spindle. A previous study showed that importin-α and -β inhibit the microtubule binding of hKid in vitro (Trieselmann et al., 2003), which supports our results. It must be noted that neither phenomena was observed in the presence of importin-α or -β alone (Fig. 3 B), demonstrating the necessity of binding with importin-β and -α in determining the subcellular localization of hKid.

Local production of Ran-GTP on mitotic chromosomes promotes the importin-β–mediated chromosome loading of hKid

In mitosis, it is well accepted that chromosome-bound RCC1, a Ran guanine nucleotide exchange factor, constitutively generates Ran-GTP, producing a high Ran-GTP concentration around mitotic chromosomes (Kalab et al., 2002, 2006). Such a high local Ran-GTP concentration is considered to be critical for liberating various mitotic factors from the inhibitory effects of importins (Harel and Forbes, 2004). Along with this scenario, one may expect that importin-β does not bind hKid in the vicinity of the chromosomes; therefore, the physiological relevance of the importin-β–mediated chromosome loading of hKid is unknown. Q69L Ran-GTP reversed the effects of importin-β (Fig. 3 A, third column); however, under physiological conditions, Ran is continuously interconverted between its GTP and GDP forms at the mitotic chromosomes because of the actions of RCC1 and RanGAP (Melchior, 2001). We therefore partially reproduced these conditions in permeabilized cells by adding Ran-GDP together with an energy source and reexamined the behavior of hKid in that setting. Although the addition of Ran-GDP to the reaction did not overtly affect the behavior of hKid with regard to the chromosome and spindle (Figs. 3 A and 4 A, compare second columns), the addition of Ran-GDP together with an energy source enhanced the chromosome loading of hKid (Fig. 4 A, fourth column). The addition of Ran-GDP and an energy source in the absence of importin-α and -β also induced weak chromosome binding of hKid (Figs. 4 A and 5 A, third column). A chromosomal factor must have mediated this binding because mutant hKid that was defective in its NLSs was able to bind the chromosomes under these conditions (Fig. 5 B). The effect observed here was Ran independent because addition of the energy source alone also induced the same level of binding (unpublished data). When Ran-GDP was replaced with T24N Ran, a mutant Ran that inhibits the production of Ran-GTP by binding to RCC1 (Klebe et al., 1995), no increase in the chromosome loading of hKid was observed (Fig. 4 B). The addition of an energy source to permeabilized cells inevitably caused depolymerization of the spindle microtubules (Fig. 4 A, third row), raising the possibility that the increase in chromosome loading seen in the fourth column of Fig. 4 A was merely caused by a shift in the spindle population to the chromosomes. This possibility is unlikely, however, because the targeting of hKid was not enhanced in all settings involving disruption of the mitotic spindle in the presence of importin-α

Published February 11, 2008

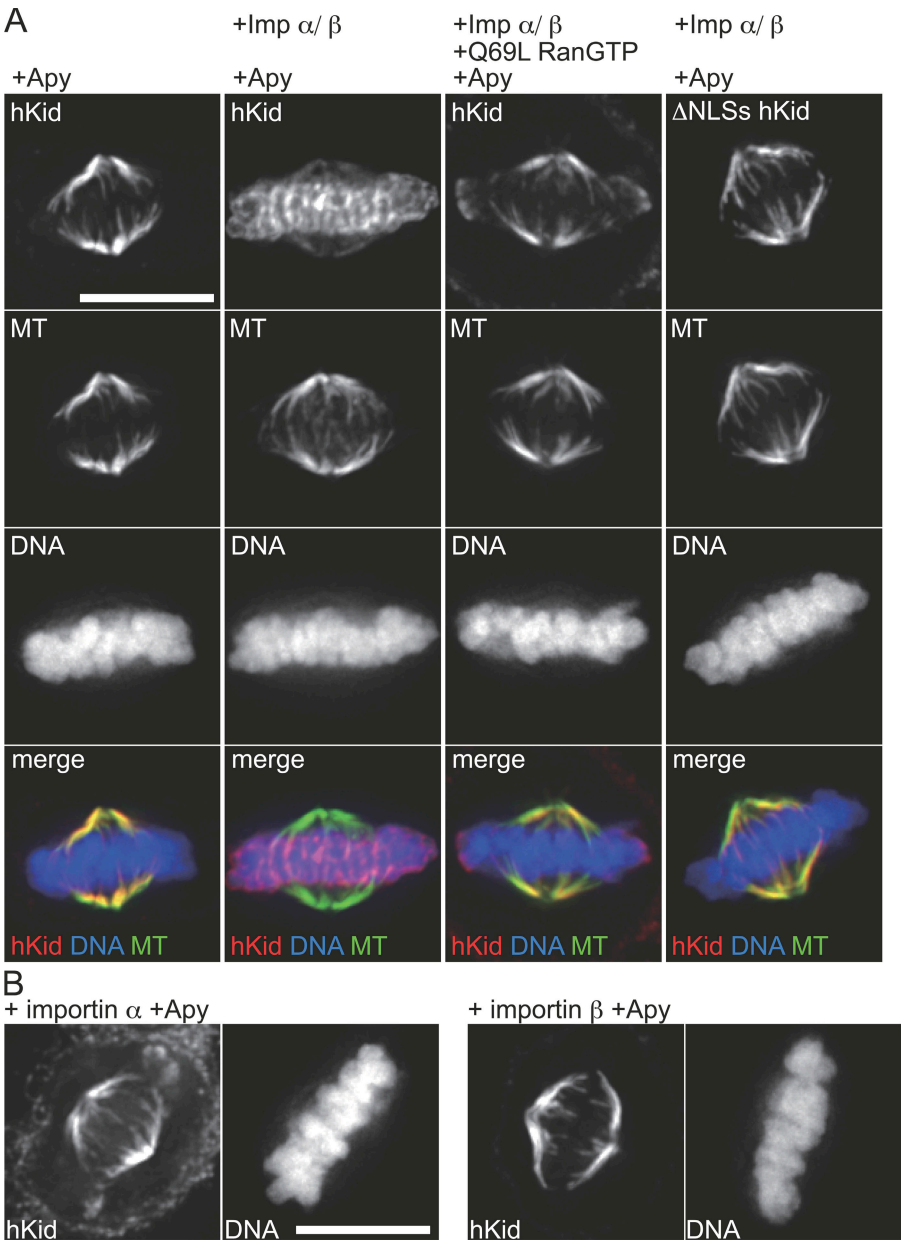

Figure 3. **Importin-α/β inhibits spindle binding but facilitates chromosome loading of hKid in digitonin-permeabilized cells.** (A) Digitonin-permeabilized mitotic HeLa cells were incubated with 0.4 μM FLAG-hKid or FLAG–ΔNLSs hKid in the absence or presence of 0.8 μM each importin-α and -β, with or without 4 μM Q69L Ran-GTP. Note that the recombinant proteins were present in excess compared with the mitotic chromosomes and mitotic spindles contained in the permeabilized cells, indicating that the reduction observed in the spindle signal of hKid upon addition of importin-α/β was caused by the inhibition of spindle binding. (B) Digitonin-permeabilized mitotic HeLa cells were incubated with 0.4 μM FLAG-hKid in the presence of either 0.8 μM importin-α or -β. All reactions were performed in the presence of apyrase, which depleted the energy source. The same results were obtained without the addition of the energy source to the reaction mixture (not depicted). After incubation, the cells were fixed and processed for indirect immunofluorescence staining to detect FLAG-hKids and the spindle microtubules, as described in Materials and methods. DNA was counterstained with DAPI. The images are projections of five deconvolved sections taken at 0.2-μm focus intervals. Bars, 10 μm.

and β (Fig. 4 B, right; and Fig. 5). Collectively, hKid seems to be targeted as a complex, with importin-α and -β, to the vicinity of mitotic chromosomes where it is loaded in a Ran-GTP–dependent manner.

To examine the loading of hKid onto chromosomes without the interference of spindle microtubules, the experiments shown in Fig. 4 A were repeated in nocodazole-treated permeabilized cells. As shown in Fig. 5 A, importin-α and -β clearly induced the chromosomal targeting of hKid, indicating that hKid complexed with importin-α and -β can target to chromosomes without the use of spindle microtubules. The targeting was enhanced by the addition of Ran-GDP and an energy source, confirming that local production of Ran-GTP positively affects the importin-β–mediated chromosome loading of hKid. None of the effects mediated by importin-α and -β were observed with hKid lacking functional NLSs (Fig. 5 B), which confirms the specificity of these observations.

Ran-GTP production induces local cargo release at chromosomes and supports the chromosomal accumulation of hKid

To understand how local Ran-GTP production stimulates the importin-β–mediated chromosome loading of hKid, the behavior of importin-α and -β during this process was dissected using CFP-tagged importin-α and YFP-tagged importin-β, both of which are capable of mediating the nuclear import of NLS-containing substrates (unpublished data). As shown in Fig. 6, importin-α and -β were cotargeted to mitotic chromosomes with hKid. The reaction was specifically induced upon the formation of a complex with hKid because a general NLS-containing cargo, SV40 T-antigen NLS conjugate, did not induce the same targeting (Fig. 6, first column). In the presence of Ran-GDP and an energy source, importin-β was released from the mitotic chromosomes (Fig. 6, third column). The addition of CAS, an export factor for importin-α (Kutay et al., 1997), released a significant amount of

Published February 11, 2008

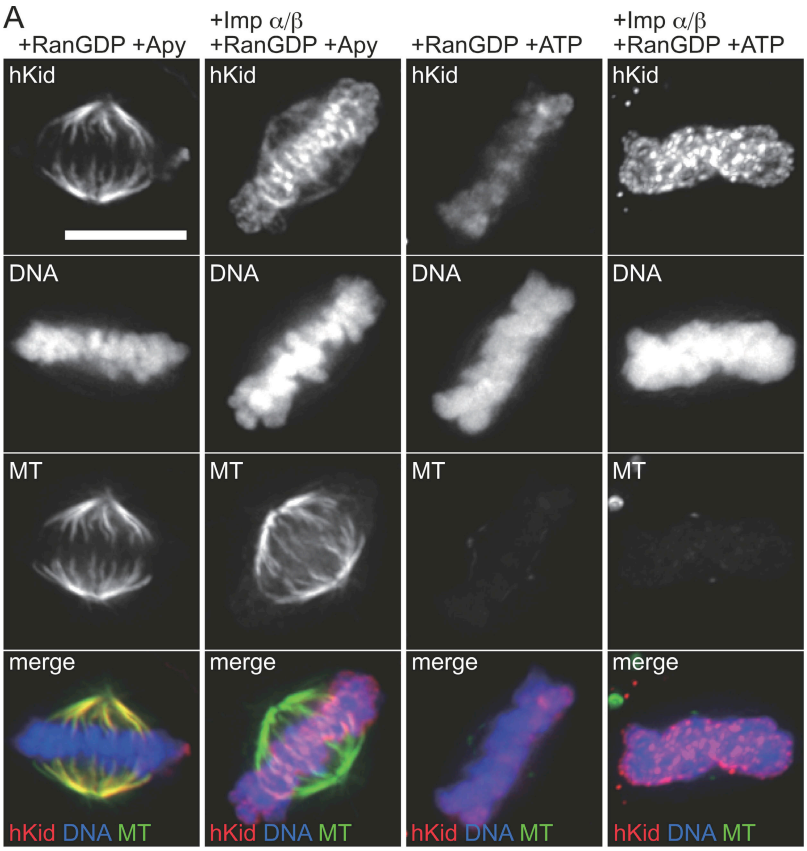

Figure 4. **Importin-β–mediated chromosome loading of hKid is promoted by the production of Ran-GTP.** (A) Digitonin-permeabilized mitotic HeLa cells were incubated with 0.4 μM FLAG-hKid in the presence or absence of 0.8 μM importin-α, 0.8 μM importin-β, and 4 μM RanGDP with or without an energy source. (B) Digitonin-permeabilized mitotic HeLa cells were incubated with 0.4 μM FLAG-hKid in the presence or absence of 0.8 μM importin-α, 0.8 μM importin-β, and 4 μM RanGDP or 4 μM T24N Ran with an energy source. After incubation, the cells were fixed and subjected to indirect immunofluorescence staining and the images were processed as described in Fig 3. Bars, 10 μm. Quantification of the fluorescent intensities of the images taken under the same conditions showed that the chromosomal accumulation of FLAG-hKid was reduced to 57% when Ran-GDP was replaced with T24N Ran.

Published February 11, 2008

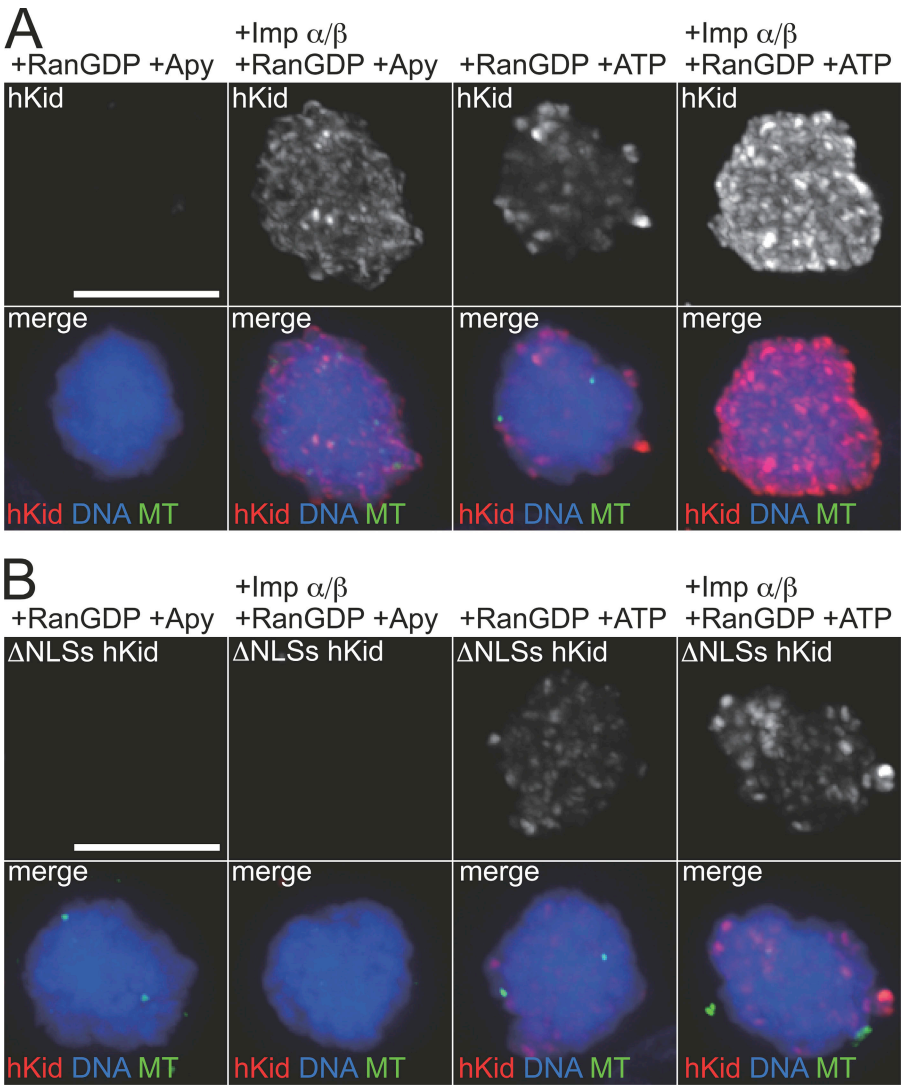

Figure 5. **The effect of importin-α/β and Ran-GTP production on hKid chromosomal loading is independent of the mitotic spindle.** HeLa cells treated with 2 μM nocodazole for 2 h were permeabilized with digitonin and then incubated with 0.4 μM FLAG-hKid or 0.4 μM FLAG–ΔNLSs hKid in the presence or absence of 0.8 μM importin-α, 0.8 μM importin-β, and 4 μM Ran-GDP with or without an energy source. After incubation, the cells were fixed and subjected to indirect immunofluorescence staining. The images are projections of 46 deconvolved sections taken at 0.2-μm focus intervals. Bars, 10 μm.

importin-α from the mitotic chromosomes (Fig. 6, fourth column), whereas hKid remained bound. These results indicate that a transient association of hKid with importin-α and -β is necessary for the initial targeting of hKid to mitotic chromosomes and that local Ran-GTP–mediated cargo release promotes the efficient accumulation of hKid at mitotic chromosomes.

Disruption of the Ran GTPase cycle affects the mitotic localization of endogenous hKid in living cells

We next assessed whether disruption of the Ran GTPase cycle actually affects the mitotic localization of endogenous hKid in living cells. For this, Ran mutants defective in the GTPase cycle were overexpressed in HeLa cells in combination with cell cycle synchronization so that cells in the first round of mitosis after transfection could be efficiently observed (see Materials and methods). The localization of endogenous hKid in these cells was examined by immunostaining. As shown in Fig. 7, overexpression of Q69L Ran, a Ran mutant defective in GTP hydrolysis, or T24N Ran, which inhibits RCC1 activity, both reduced the chromosome signals of hKid more markedly than overexpression of wt Ran. Although Ran expression was extremely variable from cell to cell, the overexpressed Ran proteins altered the behavior of hKid in a manner dependent on the mutant type rather than the level of expression (Fig. S3, available at http://www.jcb.org/cgi/content/full/jcb.200708003/DC1). These data are consistent with the in vitro observations shown in Fig. 4, and they further support the notion that the Ran GTPase cycle contributes to the chromosome loading of hKid.

Discussion

In this study, we found that importin-β and Ran actively mediate the chromosome loading of hKid during mitosis. We first identified the NLSs of hKid (Fig. 1) and established cell lines that stably expressed wt or NLS-deficient hKid fused to Venus (Fig. 2 A). We then carefully compared the behavior of the two proteins in live cells by FRAP and FLIP and found that hKid with functional NLSs had greater affinity for mitotic chromosomes but lower affinity for the mitotic spindle (Fig. 2). To dissect these phenomena more precisely, we examined how nucleocytoplasmic transport factors affect the mitotic behavior

Published February 11, 2008

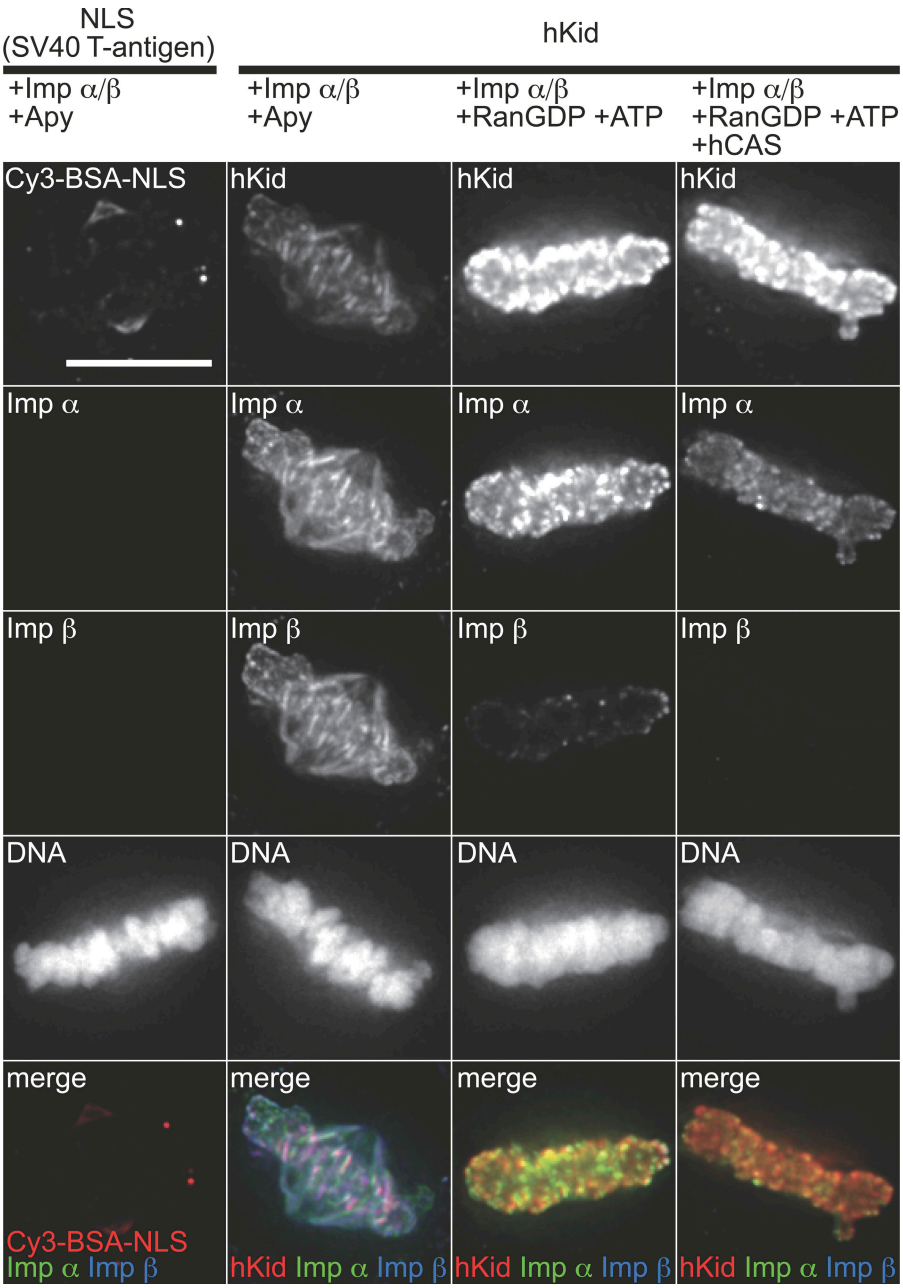

Figure 6. **Ran-GTP production induces local cargo release at chromosomes and supports the chromosomal accumulation of hKid.** Digitonin-permeabilized mitotic HeLa cells were incubated with 0.4 μM FLAG-hKid or 0.4 μM Cy3-BSA-NLS in the presence of 0.4 μM CFP–importin-α and 0.4 μM YFP–importin-β, with or without 4 μM Ran-GDP, an energy source, and 1.7 μM CAS. After incubation, the cells were fixed and subjected to indirect immunofluorescence staining. The images were processed as described in Fig 3. Bar, 10 μm.

of hKid using digitonin-permeabilized mitotic cells (Fig. 3). In permeabilized cells, we found that chromosome loading of hKid could be reconstituted only in the presence of transport factors (Figs. 3–6), leading to the model depicted in Fig. 8. In this model, hKid is recruited to the vicinity of the chromosomes as a ternary complex with importin-α and -β and then deposited onto the chromosomes by the GTP-exchange reaction of Ran, which is mediated locally by chromosomal RCC1. Dissociation of importin-β occurs through the chromosomal generation of Ran-GTP, whereas CAS is required for the dissociation of importin-α. Based on these phenomena, we propose that importin-α and -β not only inhibit the activity of certain proteins, including SAFs, but also actively recruit proteins to chromosomes. With regard to the deposition of hKid on chromosomes, the Ran-GTP–induced release of importin-α and -β may be critical, as has been shown in the activation of other SAFs (Harel and Forbes, 2004).

What is the advantage of hKid being subjected to regulation by importins? Because the overexpression of hKid is extremely cytotoxic, proper control of the amount and localization of the protein during mitosis is probably important. Knockdown of endogenous hKid using siRNA duplexes targeted to the 3′-UTR unexpectedly up-regulated the expression of Venus-hKid in stably transformed cells (unpublished data), implying that the amount of hKid in cells is determined via an unknown mechanism. Besides the overall concentration of hKid, the proportion of hKid at the mitotic spindle and chromosomes is assumed to be important for hKid function because its affinity for spindle microtubules is regulated by cyclin B/cdc-2 kinase (Ohsugi et al., 2003). Importin-α and -β prevented hKid from associating with

Published February 11, 2008

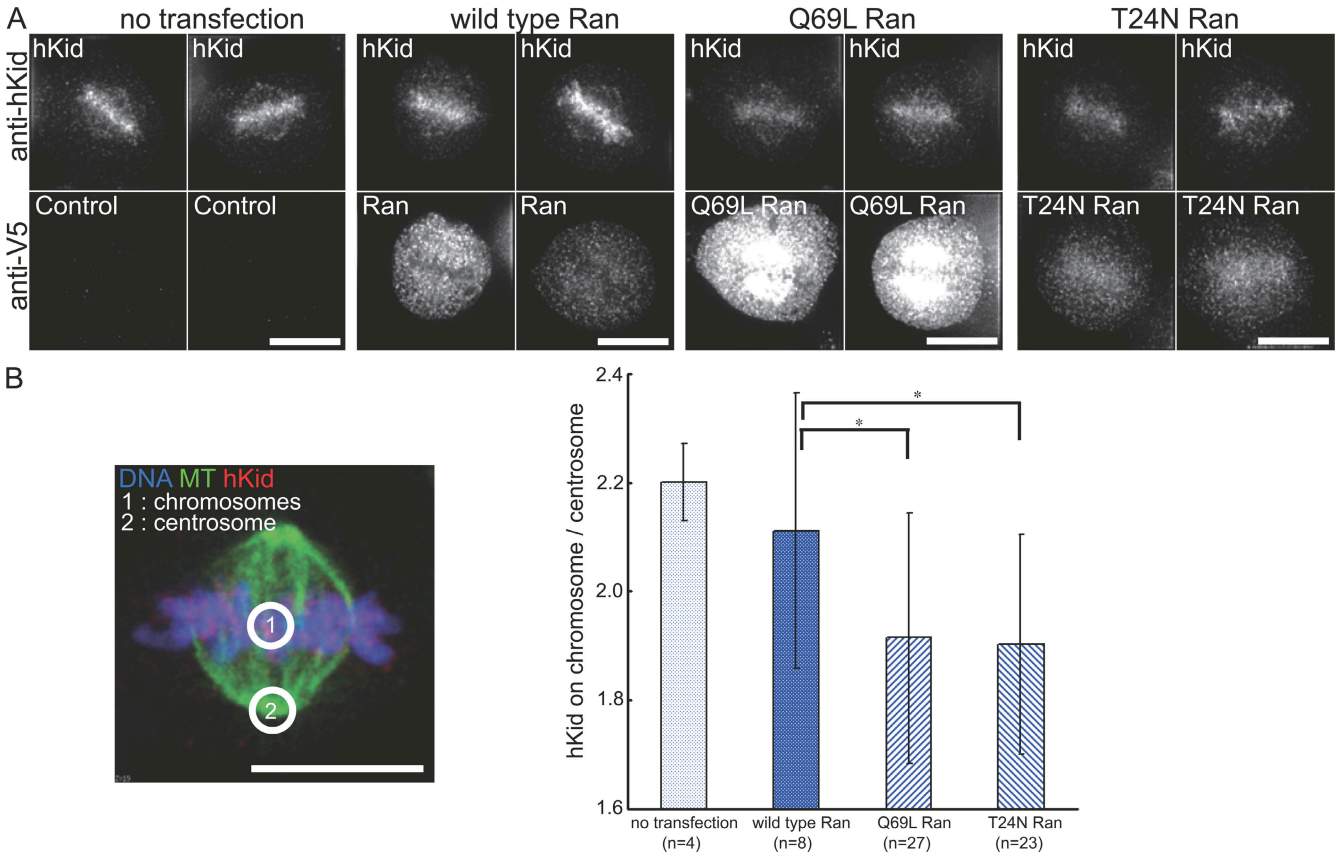

Figure 7. **Expression of mutant Ran defective in the GTPase cycle affects the mitotic localization of endogenous hKid in living cells.** (A) Synchronized HeLa cells were transfected with expression vectors encoding wt Ran, Q69L Ran, or T24N Ran as described in Materials and methods. 10 h after their release from a second thymidine block, the cells were fixed and stained for endogenous hKid and Ran. The images are projections of five deconvolved sections taken at 0.2-μm focus intervals. Bars, 10 μm. (B) Quantification of the results in A. Cells expressing the indicated Ran proteins were fixed and stained. The fluorescent intensity of hKid on the chromosomes (1) and centrosomes (2) was measured using SoftWorx software and their ratios were plotted. The values are expressed as the mean ± standard deviation. Significant differences were detected using *t* test. *, $P < 0.05$. Bar, 10 μm.

spindle microtubules and actively mediated the targeting of hKid to the chromosomes in permeabilized cells (Figs. 3 and 4), indicating that these factors tilt the dynamic equilibrium of hKid to the chromosome side.

Meanwhile, FRAP analysis revealed that the rate of turnover and the mobile fraction of Venus–ΔNLSs hKid was increased compared with that of Venus–wt hKid (Fig. 2 B). This indicates that the NLSs of hKid must play additional roles in determining the nature of the interaction of hKid with chromosomes besides affecting the dynamic equilibrium between the mitotic spindle and chromosomes.

The initial chromosomal locations to which hKid is targeted by importin-β and the subsequent sites of loading, which may be coupled with the RCC1-mediated dissociation of importin-α and -β, might be different. The chromosomal localization of hKid apparently differs depending on the presence or absence of Ran-GDP and an energy source (e.g., compare the second and fourth columns in Fig. 4 A). To further explore the molecular basis for these observations, we performed an in vitro DNA binding assay using recombinant proteins. The DNA binding activity of hKid to DNA-Sepharose was weakened by the addition of importin-α and -β (unpublished data). This indicates that the initial targeting site induced by importin-β is not naked DNA. The DNA binding site of hKid, which is necessary for its chromosomal localization in living cells (Levesque and Compton, 2001; Ohsugi et al., 2003), may also be required for subsequent deposition. Further biochemical analyses are required to understand how importins and Ran contribute to the nature of the chromosome–hKid interaction.

It is evident that hKid is able to bind chromosomes without the help of importins, based on the fact that Venus–ΔNLSs hKid was predominantly localized on mitotic chromosomes, as was Venus–wt hKid (Fig. 2 A). Our in vitro data suggest the existence of functional differences among hKid proteins depending on whether they are loaded onto chromosomes via an importin-dependent or -independent route. Because hKid cannot bind spindle microtubules without dissociating from importins, it is possible that hKid is loaded onto spindle microtubules via a chromatin-bound stage instead of being loaded onto chromosomes from the spindle. If so, the chromosomal sites onto which hKid is loaded via an importin-dependent mechanism could serve as microtubule nucleating/attachment sites.

The notion that the NLSs of hKid contribute to its chromosomal loading is supported by all of our observations except for the FLIP data obtained in the presence of a mitotic spindle (Fig. 2 C). The data do not necessarily contradict our present

Published February 11, 2008

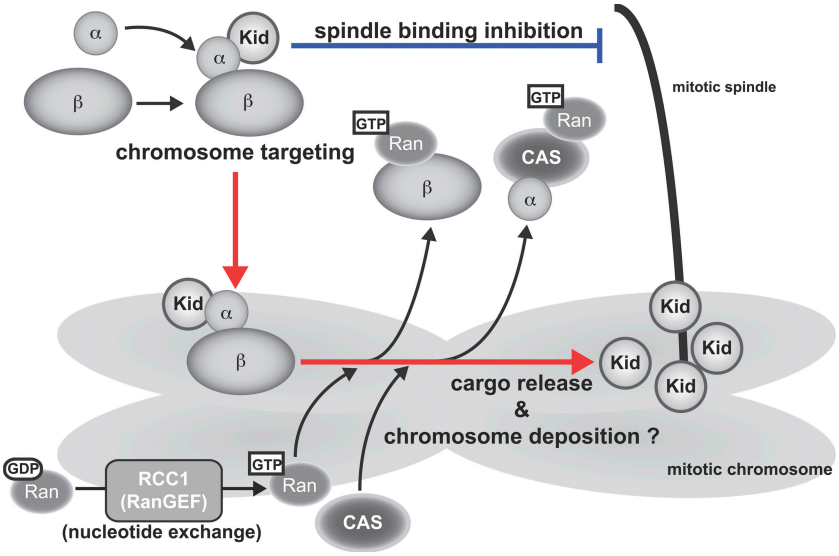

Figure 8. **Model of the importin-β–mediated chromosome loading of hKid.** The association of hKid with importin-β via importin-α triggers the initial targeting of hKid to mitotic chromosomes, whereas cargo release, mediated by the action of Ran-GTP, which is generated locally at the chromosomes, promotes the accumulation of hKid on the chromosomes. Cargo release is likely coupled with the deposition of hKid onto the chromosomes.

suggestion that hKid is loaded onto chromosomes by importins without the help of the spindle but would, rather, support our in vitro results showing that the importin–hKid interaction inhibits the binding of hKid to microtubules. The FLIP data in Fig. 2 C must be interpreted with caution, given that the ratio of the spindle population in our experimental cells was higher for Venus–ΔNLSs hKid than for Venus–wt hKid. The former was bleached with lower efficiencies than the latter when a cytosolic area of the cells was bleached, resulting in an apparent loss of differences in our FLIP measurements.

An important point suggested by our results is that the release of hKid from importin-α and -β must occur locally on chromosomes in order for hKid to be deposited. Given that Q69L Ran (mimicking high Ran-GTP everywhere) and T24N Ran (inhibiting the production of Ran-GTP by RCC1) were unable to mimic the effect of wt Ran (Figs. 3 A and 4 B), local chromosomal production of Ran-GTP is indeed critical for the release of hKid from importin-α and -β. Our data do not deny the well-accepted concept of a high Ran-GTP concentration around the chromosomes; instead, they raise the possibility that the production of Ran-GTP at chromosomes is transient and, therefore, the gradient may be quite flexible when examined in terms of both time and space. In addition, we must consider the differences in affinity that may exist between different cargos (mitotic Ran effectors) and transport carriers, as well as between transport carriers and Ran-GTP, to understand more precisely how mitosis is conducted spatially and temporally. Depending on the local shape of the gradient and the concentration of Ran-GTP required to dissociate the importin–effector complex, this gradient might restrict each effector to a specific site of action.

Our observations suggest that the general role of nucleotide turnover in Ran during mitosis is not only to release SAFs from their inhibitory importins, but also to recruit/deposit other factors to specific sites of action. In yeast, the RNA binding protein npl3p (Senger et al., 1998) and the DNA binding protein TBP (Pemberton et al., 1999) are released from their import carriers by the action of Ran-GTP, but only in the presence of RNA and DNA, respectively. These data suggest that import carriers might be used for specific targeting. In another instance, the Ran-GTP/GDP cycle function in protein recruitment/deposition involves the movement of the RanGAP1–RanBP2 complex to kinetochores (Arnaoutov et al., 2005), although Crm1/exportin-1, an importin-β family nuclear export carrier, is used instead of importin-β. Although the mechanism is unknown, the formation of a ternary complex comprised of Crm1, Ran-GTP, and an NES-containing cargo is essential (Arnaoutov et al., 2005). Further dissection, possibly with the use of permeabilized cells and biochemical analysis, will allow for a comparison that may provide a general model of the recruitment of effectors to specific sites involving the Ran-GTP/GDP cycle and importin-β family proteins.

Materials and methods

Plasmid construction

hKid was amplified by PCR using primers (5′-TAATAGGATCCATGGCCGCGGGCGCTCGACGCAG-3′ and 5′-AACATCTCGAGTCAGGAGGCGCCACAGCGCTGGCC-3′) from the SuperScript HeLa cell cDNA library (Invitrogen). The product was then digested with BamHI and XhoI and cloned into the corresponding sites of pGEM7Zf(+). Mutations in the hKid NLSs (ΔNLS1, ^{400}KRAR^{403} to ^{400}AAAA^{403}; and ΔNLS2, ^{556}RKRKL^{560} to ^{556}AAGAA^{560}) were introduced using QuikChange (Stratagene) and confirmed by sequencing. For recombinant protein expression, the inserts were subcloned into the BamHI–XhoI sites of a modified version of pGEX-6P-1 (GE Healthcare) encoding the FLAG epitope DYDDDDK at the N terminus of its products, yielding pGEX-6P-1–FLAG-hKid and pGEX-6P-1–FLAG–ΔNLSs hKid. For our mammalian expression studies (Fig. 1), the inserts were subcloned into the BglII and SalI sites of pEGFP-C1 (Clontech Laboratories, Inc.). Expression clones of Venus-hKids, which were used to establish stable transformants by the Flp-In system (Invitrogen), were constructed using the Multisite Gateway system (see Establishment of HeLa cells stably expressing...).

The recombinant expression vectors for importin-α (Rch1), importin-β, Ran, Q69L Ran, and CAS have been described previously (Imamoto et al., 1995a,b; Hieda et al., 1999). For expression of GST-CFP and GST-YFP, the coding sequences for ECFP and EYFP were amplified by PCR from pECFP and pEYFP (gift from A. Miyawaki, Institute of Physical and Chemical Research Brain Science Institute, Wako, Saitama, Japan), respectively, and subcloned into the BamHI site of pGEX6P-1 to produce pGEX6P-1/ECFP and pGEX6P-1/EYFP. Expression vectors for CFP–importin-α and YFP–importin-β were constructed by insertion of DNA encoding importin-α and -β into pGEX6P-1/ECFP and pGEX6P-1/EYFP, respectively. The expression vector for T24N Ran was constructed by insertion of DNA encoding T24N Ran into pQE-80L (QIAGEN).

Published February 11, 2008

Mammalian expression constructs of V5-tagged Ran were generated using the Gateway system (Invitrogen). In brief, cDNA fragments encoding wt or mutant Ran were amplified by PCR with KOD-plus polymerase (Toyobo), using previously described Ran plasmids as templates (Hieda et al., 1999) such that attB1 and attB2 were introduced at the 5′- and 3′ ends, respectively. The fragments were then subcloned into pDONR221 (Invitrogen) using BP clonase (Invitrogen) and transferred to pcDNA3.1/nV5/DEST (Invitrogen) using LR clonase (Invitrogen).

Recombinant proteins, reagents, and antibodies

Expression vectors encoding N-terminal GST- and FLAG-tagged wt hKid and ΔNLSs hKid were transformed into *Escherichia coli* strain BL21 (DE3). Expression was induced by the addition of 0.1 mM IPTG followed by 18 h of incubation at 20°C. The cells were then harvested by centrifugation and disrupted in buffer A (50 mM Tris-HCl, pH 8.3, 500 mM NaCl, 2 mM DTT, and 200 μM PMSF) by freeze thawing and sonicating. The clarified supernatant was incubated with glutathione–Sepharose 4B (GE Healthcare) for 2.5 h at 4°C, and the bound proteins were eluted with 20 mM glutathione dissolved in buffer B (50 mM Tris-HCl, pH 8.8, 500 mM NaCl, 2 mM DTT, 0.1% Tween 20, and 1 μg/ml each aprotinin, leupeptin, and pepstatin A) after extensive washing of the Sepharose beads with buffer P (50 mM Tris-HCl, pH 8.3, 500 mM NaCl, 2 mM DTT, 0.1% Tween 20, and 1 μg/ml each aprotinin, leupeptin, and pepstatin A). GST was cleaved off by incubation with PreScission protease for 36 h at 7°C, and hKid was purified on a MonoS column (GE Healthcare) using a linear gradient of 0.25–1.0 M NaCl dissolved in buffer C (20 mM Hepes, pH 7.3, and 2 mM DTT). The peak fractions containing each recombinant protein were collected. After adjusting the NaCl concentration to 1 M, the proteins were concentrated by ultrafiltration on Microcon YM-30 columns (Amicon) and desalted using a PD10 column (GE Healthcare) equilibrated with buffer D (20 mM Hepes, pH 7.3, 400 mM NaCl, 2 mM DTT, and 1 μg/ml each aprotinin, leupeptin, and pepstatin A).

The expression vector encoding T24N Ran, N-terminally tagged with 6×His, was transformed into *E. coli* strain JM109. Expression was induced by the addition of 1 mM IPTG followed by incubation for 18 h at 20°C. The cells were then harvested by centrifugation and disrupted by sonication in 50 mM KPO_4 buffer, pH 8.0, 300 mM NaCl, 1 mM β-mercaptoethanol, 100 μM PMSF, 1 μg/ml each aprotinin, leupeptin, and pepstatin A, and 1 mg/ml lysozyme (Wako). The clarified supernatant was incubated with Ni-NTA agarose (QIAGEN) for 4 h at 4°C, and the bound proteins were eluted with 250 mM imidazole dissolved in buffer E (20 mM KPO_4, pH 7.0, 0.5 mM $MgCl_2$, 0.5% glycerol, and 1 mM β-mercaptoethanol) after extensive washing of the Sepharose beads with buffer E. The His-T24N Ran proteins were purified on MonoQ columns (GE Healthcare) using a linear gradient of 0.02–0.5 M KPO_4. The peak fractions containing each recombinant protein were collected. The proteins were then concentrated by ultrafiltration on Microcon YM-10 columns (Amicon) and desalted using PD10 columns (GE Healthcare) equilibrated with buffer F (20 mM KPO_4, pH 7.0, 0.5 mM $MgCl_2$, 2 mM DTT, 1 mg/ml BSA, and 1 μg/ml each aprotinin, leupeptin, and pepstatin A).

Recombinant importin-α, importin-α ED (E396R and D192K; Conti et al., 1998; Gruss et al., 2001), importin-β, CFP–importin-α, and YFP–importin-β were expressed in *E. coli* and purified as previously described (Kose et al., 1997). wt Ran-GDP, Q69L Ran-GTP, and CAS were expressed in *E. coli* and purified as previously described (Hieda et al., 1999). SV40 T-antigen NLS-conjugated BSA was prepared using the synthetic peptide CYGGPKKKRKVED as previously described (Imamoto et al., 1995b).

The antibodies used in this study include the following: anti-FLAG mouse monoclonal antibodies (Sigma-Aldrich) for detecting recombinant FLAG-hKid (Figs. 1 and 3–6); anti-Kid rabbit antibodies (Tokai et al., 1996; Figs. 2 and 7); anti-V5 monoclonal antibody (Invitrogen) for detection of overexpressed V5-tagged Ran (Fig. 7); and FITC-conjugated DM1α (Sigma-Aldrich) for the experiments described in Figs. 3–7. The secondary antibodies used include the following: Cy3-conjugated donkey anti–mouse polyclonal antibodies (Jackson ImmunoResearch Laboratories); Alexa 488–conjugated goat anti–rabbit polyclonal antibodies (Invitrogen); and Alexa 647–conjugated goat anti–mouse polyclonal antibodies (Invitrogen).

Cell culture and transfection

HeLa cells were cultured in DME containing 10% heat inactivated FBS at 37°C in a humidified incubator with 5% CO_2. HeLa cells stably expressing Venus–wt hKid or Venus–ΔNLSs hKid were established by selection with medium containing 200 μg/ml hygromycin B.

For the permeabilized cell-free assay described in Figs. 1 and 3–6, asynchronous HeLa cells were plated on 8-well multitest slides (ICN) 24–36 h before use. For the microinjection studies in Fig. 1, asynchronous cells were plated on 35-mm glass-bottom dishes. For FRAP and FLIP (Fig. 2 and Fig. S2), HeLa cells stably expressing Venus–wt hKid or Venus–ΔNLSs hKid were plated on 35-mm glass-bottom dishes at a concentration of 2×10^5 cells/dish 36–48 h before analysis. Cells were treated with 2 μM nocodazole for 2 h before FLIP analysis. For the experiments described in Fig. 7, transfection was combined with synchronization of the cells by a double thymidine block. In brief, HeLa cells were seeded on poly-L-lysine–coated coverslips in 35-mm dishes at a concentration of 0.5×10^5 cells/dish. 1 d later, the cells were treated with 2 mM thymidine for 16 h and released into fresh medium for 8 h. The cells were transfected using Lipofectamine 2000 (Invitrogen), according to the manufacturer's instructions, 4 h into the release period. A second thymidine block was applied for 16 h. The cells were then released into fresh medium for 10 h, fixed, and processed for immunofluorescence.

FRAP and FLIP analysis

FRAP and FLIP were performed using a quantifiable laser module (50 mW, 488-nm solid-state laser) and restoration microscopy system (DeltaVision RT; Applied Precision; Andrews et al., 2004) equipped on a microscope (IX-71; Olympus) with a 60× apochromatic objective lens (Olympus). During analysis, the cells were maintained in phenol red–freeDME containing 25 mM Hepes (Invitrogen) and 10% FBS at 37°C in a live-cell imaging chamber (MI-IBC; Olympus).

FRAP analysis. The laser was focused to a diffraction-limited spot on the mitotic chromosomes, and spot bleaching was performed with a single 100-ms stationary pulse at 30% laser power. In metaphase cells, the first image was acquired ∼20 ms after bleaching. Next, 50 images were acquired every 100 ms in "As Fast As Possible" mode. In anaphase cells, images were acquired every 1.2 or 1.6 s after bleaching for 60 s. Fluorescence recovery in the bleached spots was calculated using SoftWorx software (Applied Precision) and Excel (Microsoft) as follows: the mean intensity values at time t of a bleached chromosomal spot (a_t), a nonbleached chromosomal spot (b_t), and a nonchromosomal spot (background, c_t) were determined, and relative fluorescence recovery was calculated as $(a_t - c_t)/(b_t - c_t)$. Each value was normalized to its value before bleaching. $t_{1/2}$ was calculated according to $t_{1/2} = \ln(2)/k$, where k is the time constant for a single exponential recovery model. The recovery percentage was taken as the final plateau intensity. All recovery measurements were well fitted by single exponential recovery kinetics (Kaleidagraph version 4.0; Synergy Software).

FLIP analysis. A spot outside the chromosomes and mitotic spindle was irradiated for bleaching. The cells were treated with 2 μM nocodazole for 2 h before analysis where indicated. Laser irradiation for 1 s and subsequent image acquisition was repeated every 5 s for 35 cycles. Fluorescence intensity in the nonirradiated spot was measured as a function of time with bleaching. Similar to our FRAP analysis, the mean intensity values at time t of a single chromosomal spot before (b_{pre}) and during (b_t) irradiation and a spot outside the cells before (c_{pre}) and during (c_t) irradiation (background) were obtained, and relative fluorescence loss was calculated as $(b_t - c_t)/(b_{pre} - c_{pre})$. $t_{1/2}$ was calculated according to $t_{1/2} = \ln(2)/k$, where k is the time constant for a single exponential loss model. All loss measurements were well fitted by single exponential loss kinetics (Kaleidagraph version 4.0).

Digitonin-permeabilized cell-free assay and protein detection

Digitonin-permeabilized HeLa cells were prepared as previously described (Adam et al., 1990; Kose et al., 1997). In brief, cells grown on 8-well multitest slides were permeabilized with 40 μg/ml digitonin (EMD) in ice-cold transport buffer (TB: 20 mM Hepes, pH 7.3, 110 mM KOAc, 2 mM $MgCl_2$, 5 mM NaCl, 0.5 mM EGTA, 1 mM DTT, and 1 μg/ml each aprotinin, leupeptin, and pepstatin A) for 5 min. After removal of the buffer, those cells in interphase were subjected to a transport assay (Fig. 1), whereas those cells in mitosis were subjected to the assay described in Figs. 3–6. All reactions were performed using bacterially expressed purified recombinant FLAG-hKids, importin-α, importin-β, Ran-GDP, Q69L Ran-GTP, His-T24N Ran, CFP–importin-α, YFP–importin-β, and CAS at the concentrations indicated in the figure legends. An ATP regenerating system (energy source: 1 mM ATP, 5 mM creatine phosphate, and 20 U/ml creatine phosphokinase) or 0.1 U/μl apyrase (energy source depletion) was added to the reaction mixture as indicated in the figure legends. After incubation for 20 min at 30°C, the cells were fixed with 3.7% formaldehyde in TB and treated with 0.2% Triton X-100 for 5 min, and then subjected to indirect immunofluorescence for FLAG-hKids (anti-FLAG monoclonal antibody combined with Cy3-conjugated secondary antibodies) and spindle microtubule (FITC-conjugated DM1α) detection. DNA was counterstained with DAPI in all experiments. Images were acquired as

Published February 11, 2008

0.2-µm sections using a charge-coupled device camera (Roper Scientific) with a microscope (IX-71) through a 60× apochromatic objective lens and processed with a microscope system (Delta Vision RT; Applied Precision). The images were deconvolved and projected using SoftWorx software.

Solution binding assay

Recombinant proteins were incubated in binding buffer (20 mM Hepes, pH 7.3, 100 mM NaCl, 1 mM DTT, 0.1% Tween 20, 0.1% ovalbumin, and 1 µg/ml each aprotinin, leupeptin, and pepstatin A) as described in the figure legends for 1 h on ice, followed by incubation with glutathione-Sepharose beads for 30 min at 4°C with rotation. After incubation, the beads were collected by centrifugation and washed three times in binding buffer without ovalbumin. The bound proteins were analyzed by SDS-PAGE and stained with Coomassie brilliant blue.

Establishment of HeLa cells stably expressing Venus–wt hKid or Venus–ΔNLSs hKid under the control of the EF1α promoter

Expression clones of Venus–wt hKid (pFRT/V5-B1-$P_{EF1\alpha}$-B6-SDK-Venus-B4-hKid-*B6-*Bgl*II-B2) and Venus–ΔNLSs hKid (pFRT/V5-B1-$P_{EF1\alpha}$-B6-SDK-Venus-B4-hKid(ΔNLSs)-*B6-*Bgl*II-B2) were constructed using the Multisite Gateway system (Sasaki et al., 2004) as follows. The entry clones pENTR-L1-$P_{EF1\alpha}$-L6 and pENTR-R6-SDK-Venus-L4 were constructed as previously described (Yahata et al., 2005). pENTR-R4-hKid-*L6 was constructed by a BP reaction using pDONR-P4rP6 (Sasaki et al., 2004) and *att*B4r-hKid-**att*B6, which was amplified by *att*B-PCR with the primers B4r-hKid-Fw (5′-GGGGCAACTTTTCTATACAAAGTTGATGGCCGCGGGCGGCTC-3′) and B6*-hKid-Rv (5′-GGGGCAACTTTGTATTAAAAAGTTGTCAGGAGGCGCCACAGCG-3′) using pGEX-6P-1-FLAG-hKid as the template. pENTR-R4-hKid(ΔNLSs)-*L6 was constructed by exchanging the 1,686-bp MluI–XbaI fragment of pENTR-R4-hKid-*L6 with the corresponding fragment of pGEX-6P-1-FLAG-hKid(ΔNLSs). pENTR-R6-*Bgl*II-L2 was constructed by a BP reaction using pDONR-P6rP2 (Sasaki et al., 2004) and the double-stranded oligo *att*B6r-*Bgl*II-*att*B2 (5′-GGGGCAACTTTTTAATACAAAGTTGAGATCTCAGCTTTCTTGTACAAAGTGGCCCC-3′). The five entry clones were reacted with the destination vector pFRT/V5-DEST to construct the expression clones Venus–wt hKid and Venus–ΔNLSs hKid (Yahata et al., 2005). Using the resultant clones, stable transformants were established using the Flp-In system as described previously (Yahata et al., 2005).

Online supplemental material

Fig. S1 shows that hKid is transported into the nucleus via the importin-α/β transport pathway in digitonin-permeabilized HeLa cells. Fig. S2 shows fluorescence recovery of Venus–wt hKid and Venus–ΔNLSs hKid on mitotic chromosomes in living cells in more detail. Fig. S3 shows several images of hKid in mitotic cells overexpressing Ran and mutant Ran at various levels. Online supplemental material is available at http://www.jcb.org/cgi/content/full/jcb.200708003/DC1.

We thank Dr. Miyawaki for his generous gift of Venus cDNA and CFP cDNA.

This work was supported by Grants-in-Aid from the Ministry of Education, Culture, Sports, Science and Technology of Japan and by funds from the Institute of Physical and Chemical Research Bioarchitect Research Project, Chemical Biology Project, and Grants-in-Aid President's Discretionary Fund (N. Imamoto), and the Directors Fund of the Institute of Physical and Chemical Research Discovery Research Institute (M. Takagi).

Submitted: 1 August 2007
Accepted: 17 January 2008

References

Adam, S.A., and L. Gerace. 1991. Cytosolic proteins that specifically bind nuclear location signals are receptors for nuclear import. *Cell.* 66:837–847.

Adam, S.A., R.S. Marr, and L. Gerace. 1990. Nuclear protein import in permeabilized mammalian cells requires soluble cytoplasmic factors. *J. Cell Biol.* 111:807–816.

Andrews, P.D., Y. Ovechkina, N. Morrice, M. Wagenbach, K. Duncan, L. Wordeman, and J.R. Swedlow. 2004. Aurora B regulates MCAK at the mitotic centromere. *Dev. Cell.* 6:253–268.

Antonio, C., I. Ferby, H. Wilhelm, M. Jones, E. Karsenti, A.R. Nebreda, and I. Vernos. 2000. Xkid, a chromokinesin required for chromosome alignment on the metaphase plate. *Cell.* 102:425–435.

Arnaoutov, A., Y. Azuma, K. Ribbeck, J. Joseph, Y. Boyarchuk, T. Karpova, J. McNally, and M. Dasso. 2005. Crm1 is a mitotic effector of Ran-GTP in somatic cells. *Nat. Cell Biol.* 7:626–632.

Blower, M.D., M. Nachury, R. Heald, and K. Weis. 2005. A Rae1-containing ribonucleoprotein complex is required for mitotic spindle assembly. *Cell.* 121:223–234.

Caudron, M., G. Bunt, P. Bastiaens, and E. Karsenti. 2005. Spatial coordination of spindle assembly by chromosome-mediated signaling gradients. *Science.* 309:1373–1376.

Chi, N.C., E.J. Adam, and S.A. Adam. 1995. Sequence and characterization of cytoplasmic nuclear protein import factor p97. *J. Cell Biol.* 130:265–274.

Ciciarello, M., R. Mangiacasale, and P. Lavia. 2007. Spatial control of mitosis by the GTPase Ran. *Cell. Mol. Life Sci.* 64:1891–1914.

Conti, E., M. Uy, L. Leighton, G. Blobel, and J. Kuriyan. 1998. Crystallographic analysis of the recognition of a nuclear localization signal by the nuclear import factor karyopherin alpha. *Cell.* 94:193–204.

Ems-McClung, S.C., Y. Zheng, and C.E. Walczak. 2004. Importin alpha/beta and Ran-GTP regulate XCTK2 microtubule binding through a bipartite nuclear localization signal. *Mol. Biol. Cell.* 15:46–57.

Franz, C., R. Walczak, S. Yavuz, R. Santarella, M. Gentzel, P. Askjaer, V. Galy, M. Hetzer, I.W. Mattaj, and W. Antonin. 2007. MEL-28/ELYS is required for the recruitment of nucleoporins to chromatin and postmitotic nuclear pore complex assembly. *EMBO Rep.* 8:165–172.

Funabiki, H., and A.W. Murray. 2000. The *Xenopus* chromokinesin Xkid is essential for metaphase chromosome alignment and must be degraded to allow anaphase chromosome movement. *Cell.* 102:411–424.

Gorlich, D., and U. Kutay. 1999. Transport between the cell nucleus and the cytoplasm. *Annu. Rev. Cell Dev. Biol.* 15:607–660.

Gorlich, D., S. Prehn, R.A. Laskey, and E. Hartmann. 1994. Isolation of a protein that is essential for the first step of nuclear protein import. *Cell.* 79:767–778.

Gorlich, D., S. Kostka, R. Kraft, C. Dingwall, R.A. Laskey, E. Hartmann, and S. Prehn. 1995. Two different subunits of importin cooperate to recognize nuclear localization signals and bind them to the nuclear envelope. *Curr. Biol.* 5:383–392.

Gruss, O.J., R.E. Carazo-Salas, C.A. Schatz, G. Guarguaglini, J. Kast, M. Wilm, N. Le Bot, I. Vernos, E. Karsenti, and I.W. Mattaj. 2001. Ran induces spindle assembly by reversing the inhibitory effect of importin alpha on TPX2 activity. *Cell.* 104:83–93.

Harel, A., and D.J. Forbes. 2004. Importin beta: conducting a much larger cellular symphony. *Mol. Cell.* 16:319–330.

Hetzer, M., O.J. Gruss, and I.W. Mattaj. 2002. The Ran GTPase as a marker of chromosome position in spindle formation and nuclear envelope assembly. *Nat. Cell Biol.* 4:E177–E184.

Hieda, M., T. Tachibana, F. Yokoya, S. Kose, N. Imamoto, and Y. Yoneda. 1999. A monoclonal antibody to the COOH-terminal acidic portion of Ran inhibits both the recycling of Ran and nuclear protein import in living cells. *J. Cell Biol.* 144:645–655.

Imamoto, N. 2000. Diversity in nucleocytoplasmic transport pathways. *Cell Struct. Funct.* 25:207–216.

Imamoto, N., T. Shimamoto, S. Kose, T. Takao, T. Tachibana, M. Matsubae, T. Sekimoto, Y. Shimonishi, and Y. Yoneda. 1995a. The nuclear pore-targeting complex binds to nuclear pores after association with a karyophile. *FEBS Lett.* 368:415–419.

Imamoto, N., T. Shimamoto, T. Takao, T. Tachibana, S. Kose, M. Matsubae, T. Sekimoto, Y. Shimonishi, and Y. Yoneda. 1995b. In vivo evidence for involvement of a 58 kDa component of nuclear pore-targeting complex in nuclear protein import. *EMBO J.* 14:3617–3626.

Kalab, P., K. Weis, and R. Heald. 2002. Visualization of a Ran-GTP gradient in interphase and mitotic *Xenopus* egg extracts. *Science.* 295:2452–2456.

Kalab, P., A. Pralle, E.Y. Isacoff, R. Heald, and K. Weis. 2006. Analysis of a RanGTP-regulated gradient in mitotic somatic cells. *Nature.* 440:697–701.

Klebe, C., H. Prinz, A. Wittinghofer, and R.S. Goody. 1995. The kinetic mechanism of Ran–nucleotide exchange catalyzed by RCC1. *Biochemistry.* 34:12543–12552.

Koffa, M.D., C.M. Casanova, R. Santarella, T. Kocher, M. Wilm, and I.W. Mattaj. 2006. HURP is part of a Ran-dependent complex involved in spindle formation. *Curr. Biol.* 16:743–754.

Kose, S., N. Imamoto, T. Tachibana, T. Shimamoto, and Y. Yoneda. 1997. Ran-unassisted nuclear migration of a 97-kD component of nuclear pore–targeting complex. *J. Cell Biol.* 139:841–849.

Kutay, U., F.R. Bischoff, S. Kostka, R. Kraft, and D. Gorlich. 1997. Export of importin alpha from the nucleus is mediated by a specific nuclear transport factor. *Cell.* 90:1061–1071.

Levesque, A.A., and D.A. Compton. 2001. The chromokinesin Kid is necessary for chromosome arm orientation and oscillation, but not congression, on mitotic spindles. *J. Cell Biol.* 154:1135–1146.

Li, H.Y., and Y. Zheng. 2004. Phosphorylation of RCC1 in mitosis is essential for producing a high RanGTP concentration on chromosomes and for spindle assembly in mammalian cells. *Genes Dev.* 18:512–527.

Macara, I.G. 2001. Transport into and out of the nucleus. *Microbiol. Mol. Biol. Rev.* 65:570–594.

Maresca, T.J., H. Niederstrasser, K. Weis, and R. Heald. 2005. Xnf7 contributes to spindle integrity through its microtubule-bundling activity. *Curr. Biol.* 15:1755–1761.

Melchior, F. 2001. Ran GTPase cycle: one mechanism–two functions. *Curr. Biol.* 11:R257–R260.

Nachury, M.V., T.J. Maresca, W.C. Salmon, C.M. Waterman-Storer, R. Heald, and K. Weis. 2001. Importin beta is a mitotic target of the small GTPase Ran in spindle assembly. *Cell.* 104:95–106.

Ohsugi, M., N. Tokai-Nishizumi, K. Shiroguchi, Y.Y. Toyoshima, J. Inoue, and T. Yamamoto. 2003. Cdc2-mediated phosphorylation of Kid controls its distribution to spindle and chromosomes. *EMBO J.* 22:2091–2103.

Pemberton, L.F., J.S. Rosenblum, and G. Blobel. 1999. Nuclear import of the TATA-binding protein: mediation by the karyopherin Kap114p and a possible mechanism for intranuclear targeting. *J. Cell Biol.* 145:1407–1417.

Rasala, B.A., A.V. Orjalo, Z. Shen, S. Briggs, and D.J. Forbes. 2006. ELYS is a dual nucleoporin/kinetochore protein required for nuclear pore assembly and proper cell division. *Proc. Natl. Acad. Sci. USA.* 103:17801–17806.

Ribbeck, K., A.C. Groen, R. Santarella, M.T. Bohnsack, T. Raemaekers, T. Kocher, M. Gentzel, D. Gorlich, M. Wilm, G. Carmeliet, et al. 2006. NuSAP, a mitotic RanGTP target that stabilizes and cross-links microtubules. *Mol. Biol. Cell.* 17:2646–2660.

Ribbeck, K., T. Raemaekers, G. Carmeliet, and I.W. Mattaj. 2007. A role for NuSAP in linking microtubules to mitotic chromosomes. *Curr. Biol.* 17:230–236.

Sasaki, Y., T. Sone, S. Yoshida, K. Yahata, J. Hotta, J.D. Chesnut, T. Honda, and F. Imamoto. 2004. Evidence for high specificity and efficiency of multiple recombination signals in mixed DNA cloning by the Multisite Gateway system. *J. Biotechnol.* 107:233–243.

Sazer, S., and M. Dasso. 2000. The ran decathlon: multiple roles of Ran. *J. Cell Sci.* 113:1111–1118.

Senger, B., G. Simons, F.R. Bischoff, A. Podtelejnikov, M. Mann, and E. Hurt. 1998. Mtr10p functions as a nuclear import receptor for the mRNA-binding protein Npl3p. *EMBO J.* 17:2196–2207.

Sillje, H.H., S. Nagel, R. Korner, and E.A. Nigg. 2006. HURP is a Ran-importin beta-regulated protein that stabilizes kinetochore microtubules in the vicinity of chromosomes. *Curr. Biol.* 16:731–742.

Stewart, M. 2007. Molecular mechanism of the nuclear protein import cycle. *Nat. Rev. Mol. Cell Biol.* 8:195–208.

Tokai, N., A. Fujimoto-Nishiyama, Y. Toyoshima, S. Yonemura, S. Tsukita, J. Inoue, and T. Yamamota. 1996. Kid, a novel kinesin-like DNA binding protein, is localized to chromosomes and the mitotic spindle. *EMBO J.* 15:457–467.

Tokai-Nishizumi, N., M. Ohsugi, E. Suzuki, and T. Yamamoto. 2005. The chromokinesin Kid is required for maintenance of proper metaphase spindle size. *Mol. Biol. Cell.* 16:5455–5463.

Trieselmann, N., S. Armstrong, J. Rauw, and A. Wilde. 2003. Ran modulates spindle assembly by regulating a subset of TPX2 and Kid activities including Aurora A activation. *J. Cell Sci.* 116:4791–4798.

Wiese, C., A. Wilde, M.S. Moore, S.A. Adam, A. Merdes, and Y. Zheng. 2001. Role of importin-beta in coupling Ran to downstream targets in microtubule assembly. *Science.* 291:653–656.

Wilde, A., S.B. Lizarraga, L. Zhang, C. Wiese, N.R. Gliksman, C.E. Walczak, and Y. Zheng. 2001. Ran stimulates spindle assembly by altering microtubule dynamics and the balance of motor activities. *Nat. Cell Biol.* 3:221–227.

Yahata, K., H. Kishine, T. Sone, Y. Sasaki, J. Hotta, J.D. Chesnut, M. Okabe, and F. Imamoto. 2005. Multi-gene gateway clone design for expression of multiple heterologous genes in living cells: conditional gene expression at near physiological levels. *J. Biotechnol.* 118:123–134.